Hydrocarbon binary diffusion coefficient measurements for use in combustion modeling

W. Sean McGivern, Jeffrey A. Manion *

Chemical and Biochemical Reference Data Division, National Institute of Standards and Technology, 100 Bureau Drive, Stop 8320, Gaithersburg, MD 20899-8320, United States

ABSTRACT

Recent studies have identified uncertainties in fuel diffusion coefficients as a source of significant uncertainty in combustion modeling. This paper presents accurate binary diffusion coefficients of linear hydrocarbons in helium and nitrogen at temperatures from 300 K to 723 K. Diffusion coefficients are determined using a reversed-flow gas chromatography (RF-GC) system. Earlier work in our laboratory has established the validity of this methodology for noble gases and methane under these elevated-temperature conditions, and we utilize the methodology to measure diffusion coefficients for longer chain systems of interest in combustion modeling: ethane, propane, and *n*-butane. For propane and *n*-butane in nitrogen, the present results show dramatically different (up to 16.9% deviation at the highest common temperature) diffusion coefficients than previous work in addition to extending the available temperature range. The effects of decomposition of the analyte at higher temperatures and adhesion of the analyte on the diffusion column at lower temperatures during the measurements are briefly considered but have only a small impact on the present systems.

Published by Elsevier Inc. on behalf of The Combustion Institute.

1. Introduction

The need for accurate diffusion coefficients for fuel species in combustion models has been identified in several studies [1–7]. Uncertainties in the fuel binary diffusion coefficients lead to uncertainties in model results on the same order as those from uncertainties in the rate constants of important combustion reactions [3]. Despite this need, measurements of diffusion coefficients, especially for larger molecules, have been rare and are typically taken near room temperature. We have constructed an apparatus for the study of diffusion coefficients at temperatures from 300 K to 723 K using the reversed-flow gas chromatography method (RF-GC) originally conceived by Katsanos and Karaiskakis [8,9]. This apparatus has been characterized using reference values of binary diffusion coefficients for combinations of helium, argon, and nitrogen as well as for methane in helium and nitrogen [10].

2. Specific objectives

In this paper, we describe a newly characterized system used to measure diffusion coefficients of hydrocarbons in both helium and nitrogen. Uncertainties in the measured diffusion coefficients due to temperature and pressure are discussed. We present the

diffusion coefficients for dilute ethane, propane, and *n*-butane in helium and nitrogen at temperatures ranging from 300 K to 723 K.

3. Experiment and analysis

The details of the experimental apparatus,[1] including systematic experimental uncertainties, have been described previously [10], and only a brief description is provided here. Diffusion coefficients are measured using a reversed-flow chromatographic system initially conceived by Katsanos and Karaiskakis [8].

A simplified schematic of the apparatus is shown in Fig. 1. Diffusion measurements utilize a tee of 6 mm inner diameter electro-polished stainless steel tubing (the "diffusion tee"). Diffusion of the analyte occurs in a 60.9 cm portion of the tee (the "diffusion column") in which no gas flow is present; this bisects a second 40 cm section (the "sampling column") through which a laminar flow is established. The diffusion tee is contained in a gas chromatography oven (Oven GC) that can be set to temperatures from 200 K to 723 K. The temperature of the tee is monitored with platinum resistance thermometers placed along the length of the diffusion column.

---

[1] Certain commercial materials and equipment are identified in this paper in order to specify adequately the experimental procedure. In no case does such identification imply recommendation of or endorsement by the National Institute of Standards and Technology, nor does it imply that the material or equipment is necessarily the best available for the purpose.

* Corresponding author.
E-mail addresses: sean.mcgivern@nist.gov (W.S. McGivern), jeffrey.manion@nist.gov (J.A. Manion).
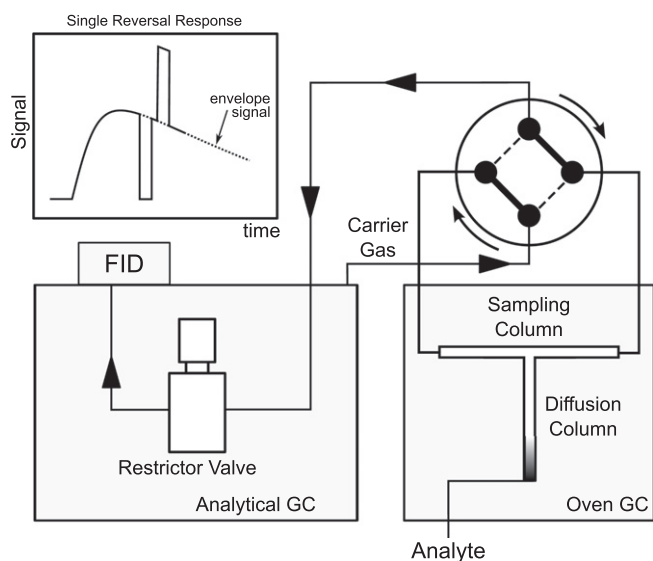
Fig. 1. Simplified experimental schematic of reversed-flow chromatography apparatus. The inset plot shows a simulated reversal signal superimposed on the envelope signal as identified in the text.

The ends of the sampling column are connected as shown to a heated four-port rotary valve. The remaining valve ports are connected to the desired carrier (bath gas) provided by a second gas chromatograph (Analytical GC) and the input of a restrictor valve. The restrictor valve is located in the Analytical GC and held at constant temperature. This setup allows a flow to be established in the sampling column that can be reversed by rotating the four-port valve. The restrictor valve is used to set the desired flow rate and corresponding pressure in the system. The pressure of the system is measured at the conclusion of each run by using the auxiliary gas electronic pressure controlled in the Analytical GC. The GC pressure measurement was calibrated with a digital pressure transducer (Mensor CPH2300, San Marcos, TX).

The end of the diffusion tee is dead-headed, providing a static column of gas throughout the diffusion column at the same time a flow is present in the sampling column. Analyte is injected at the head of the diffusion column and diffuses along its length. At the opposite end of the diffusion column, analyte is entrained in the sampling column flow as it exits the tube and is carried to the restrictor valve.

The outlet of the restrictor valve is connected to a flame ionization detector, which monitors the concentration of the analyte entrained in the sampling flow as a function of time. The resulting chromatograph has a characteristic shape that is extremely sensitive to the diffusion coefficient of the analyte [11,10]. An expression describing the resulting peak shape may be obtained by Laplace transformation of Fick's Law with appropriate boundary conditions and several simplifying assumptions [8]. The peak shape is given by

$$s \propto \frac{1}{\tau^{3/2}} \exp \frac{-L^2}{4D\tau}, \tag{1}$$

where L is the diffusion column length, D is the binary diffusion coefficient, and τ is the diffusion time after initial injection. Due to the (10 to 100) min acquisition time for typical experiments, a correction for experimental drift is desirable. To effect this, the flow through the chromatography column is periodically reversed with a four-port valve. Upon reversal, the detector output drops immediately to its baseline. After 3.6 s, the valve is rotated to its original position, and the flow continues in its original direction. The reversal allows a portion of the flowing gas in the chromatography column to pass the diffusion output twice, concentrating the sample and leading to a positive–negative peak in the output chromatogram that is superimposed on the characteristic chromatographic envelope from the diffusion column output (inset, Fig. 1). Eq. (1) applies with $\tau = t - t_h - \frac{1}{2}t_{FR}$, where t is the time the reversal was initiated measured from the analyte injection time, t_h is the holdup time for the sample to travel from the outlet of the diffusion tube to the detector, and t_{FR} is the length of time of the flow reversal [10].

Binary diffusion coefficients are extracted from the measured chromatographs by determining positive peak heights relative to the characteristic chromatographic envelope. For each reversal peak, the baseline is fit linearly between small regions surrounding the entire positive–negative set of peaks. The tip of the positive peak (typically 11 points taken at 2 Hz) is fit with a parabola and the peak value is subtracted from the linear baseline to determine the peak height, s [10]. Reversals are performed at regular intervals (typically 120 s) for the entire length of the experiment. Under specific flow and diffusion time conditions, a plot of $\ln s\tau^{3/2}$ versus $1/\tau$ will be linear with a slope of $-L^2/4D$, where L is the length of the diffusion tube, and D is the diffusion coefficient (Eq. (1)) [8,9].

To account for small uncertainties in length due to the bending of the tube and intersection of the two arms of the diffusion tee, we have previously calibrated and validated the apparatus with reference systems [10], relying on diffusion values established for the noble gases. An effective length L of 61.28 cm was derived based on an infinite-dilution value of (0.7344 ± 0.0042) cm^2 s^{-1} at 1.013 bar [12,13] for the diffusion coefficient of He in Ar at 300 K. When using this procedure the present apparatus was found to reproduce literature values for the diffusion of argon, nitrogen, and methane in helium to within 0.3% at 300 K and 1.5% at 723 K. It was observed that the length of an individual experiment must be kept sufficiently short that the $\ln s\tau^{3/2}$ versus $1/\tau$ plot produces a linear output [10], due to the failure of assumptions used to derive Eq. (1) [14,15]. At the upper end of the present temperature range, this requirement allows only a few reversals to be used in determining the diffusion coefficient, causing an increase in the uncertainty in the measured slopes. However, at these temperatures, the uncertainties in the diffusion coefficients in the present system are dominated by the temperature uncertainties. Because the diffusion occurs from a small plug of analyte at the head of a long column, the measurement occurs at a small but varying concentration. Any variation of the measured diffusion coefficients due to this concentration gradient is well within the present experimental uncertainty [16].

Finally, each diffusion coefficient is normalized linearly to 1.013 bar (1 atm) pressure for presentation; the implications of this assumption are discussed below. The present experiments were performed at pressures of (3.5–4.0) bar.

4. Results and discussion

Data for ethane (C_2H_6), propane (C_3H_8), and n-butane (C_4H_{10}) in helium and nitrogen are shown in Table 1. These data are shown graphically along with a selection of previous work in Fig. 2. The reported diffusion coefficients have been corrected to the nominal temperatures shown in the table, which represent the setting of the gas chromatography oven. Actual temperatures were measured using calibrated platinum resistance thermometers spaced along the diffusion tube. The temperature correction is derived from a fit of the individual measurements of the form

$$D = aT^m, \tag{2}$$

where a and m are fitting parameters and T is temperature in K. The parameters describing the temperature-dependence are shown in Table 2, and corrections between the measured temperatures and

Table 1
Binary diffusion coefficients for hydrocarbons in helium and nitrogen.

	Nominal, temp./K	Bath gas	D, cm^2 s^{-1}	ΔD, cm^2 s^{-1}	n	Bath gas	D, cm^2 s^{-1}	ΔD, cm^2 s^{-1}	n
C_2H_6	300	He	0.497	0.002	10	N_2	0.156	0.001	11
	350		0.642	0.001	7		0.207	0.001	8
	400		0.802	0.002	8		0.262	0.001	3
	450		0.977	0.003	4		0.322	0.002	7
	500		1.162	0.005	8		0.385	0.003	5
	550		1.361	0.008	4		0.451	0.004	9
	600		1.570	0.013	4		0.520	0.006	4
	650		1.801	0.019	5		0.595	0.008	8
	700		2.050	0.033	5		0.675	0.0013	5
	723		2.174	0.037	6		0.715	0.026	5
C_3H_8	300	He	0.404	0.001	32	N_2	0.121	0.001	9
	350		0.520	0.001	3		0.161	0.001	20
	400		0.643	0.001	4		0.205	0.001	12
	450		0.785	0.003	3		0.252	0.002	13
	500		0.936	0.004	4		0.301	0.003	4
	550		1.098	0.007	3		0.354	0.005	7
	600		1.263	0.010	3		0.409	0.007	4
	650		1.435	0.015	3		0.466	0.010	5
	700		1.640	0.027	3		0.527	0.017	5
	723		1.747	0.030	3		0.559	0.019	4
C_4H_{10}	300	He	0.338	0.002	13	N_2	[a]	[a]	[a]
	350		0.445	0.003	7		0.136	0.001	8
	400		0.554	0.002	11		0.174	0.001	9
	450		0.674	0.004	6		0.213	0.002	4
	500		0.802	0.004	10		0.256	0.002	8
	550		0.934	0.007	7		0.301	0.004	5
	600		1.074	0.011	5		0.347	0.006	4
	650		1.215	0.022	5		0.395	0.010	2
	700		1.389	0.049	5		0.453	0.016	4
	723		1.477	0.038	5		0.478	0.016	4

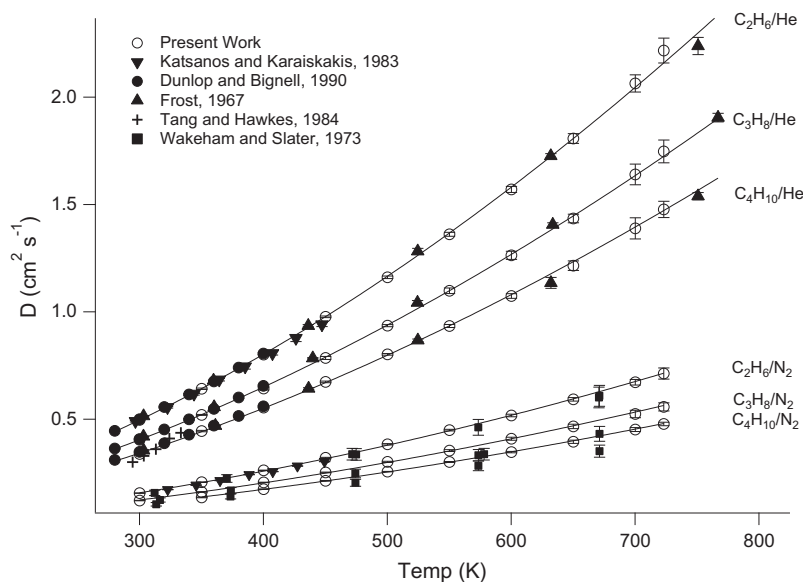[a] Data not reported. See text.

Fig. 2. Diffusion coefficients of hydrocarbons in He and N$_2$. Solid lines are fits of the form aT^m. Symbols are identified as follows: ○: this work, ▼: [11], ●: [17], ▲: [18], +: [19], ■: [16].

nominal temperatures were <0.3%. Uncertainties, indicated by Δa and Δm in the table, were derived from the corrected data, utilizing the uncertainties derived from the raw data, temperature uncertainties, and estimated systematic errors (Table 1) [10]. The value for Δa was derived from the fractional uncertainty from the fitting of the combined data in Table 1 applied to the value of a from the raw data, reported in Table 2; Δm was obtained similarly but is a linear uncertainty.

Figures 3 and 4 show deviations of measured diffusion coefficients, D, from the fits of the temperature-dependence of the present data, D_{fit} (Table 2), in helium and nitrogen, respectively. Open circles represent the present measurements, and the reported error bars are one-σ uncertainties derived from repeated determinations and estimates of systematic errors. Details of the uncertainty calculations may be found in Ref. [10]. Other symbols are previous determinations of the diffusion coefficients in other

Table 2
Parameters describing the temperature-dependence (Eq. (2)) of measured binary diffusion coefficients. a and m are the fitting parameters, and the Δ's refer to their uncertainties obtained from a weighted nonlinear fit.

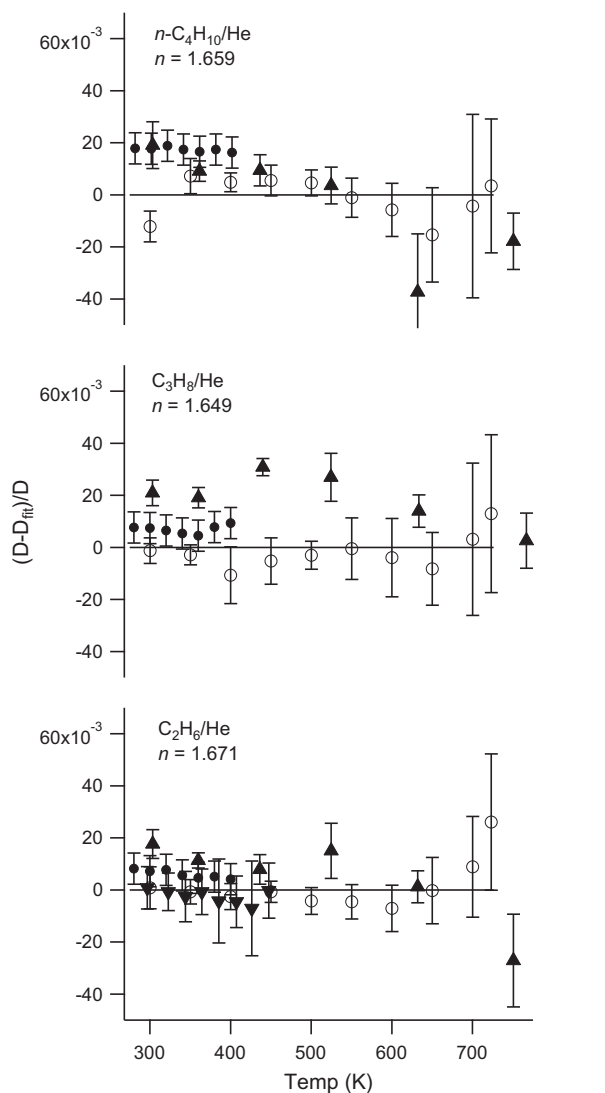| Expt.	$10^6 a/cm^2\,s^{-1}$	$10^6 \Delta a/cm^2\,s^{-1}$	m	Δm
C_2H_6/He	35.92	2.20	1.671	0.010
C_2H_6/N_2	8.63	0.55	1.720	0.010
C_3H_8/He	33.27	2.01	1.649	0.010
C_3H_8/N_2	6.68	0.54	1.723	0.014
C_4H_{10}/He	26.50	1.66	1.659	0.010
C_4H_{10}/N_2	5.76	0.58	1.721	0.016

Fig. 3. Deviations of binary diffusion coefficients for hydrocarbons in helium from fitted temperature dependence. The exponent, m, for the temperature dependence ($D = aT^m$) is shown on the figure. Error bars are one-sigma and include estimates of systematic error. Symbols are identified as follows: ○: this work, ▼: [11], ●: [17], ▲: [18], +: [19], ■: [16].

Fig. 4. Deviations of binary diffusion coefficients for hydrocarbons in nitrogen from fitted temperature dependence. The exponent, m, for the temperature dependence ($D = aT^m$) is shown on the figure. Error bars are one-sigma and include estimates of systematic error. Symbols are identified as follows: ○: this work, ▼: [11], ●: [17], ▲: [18], +: [19], ■: [16].

laboratories and are identified in Fig. 2 and discussed in the following sections.

4.1. Diffusion of hydrocarbons in helium

The simple temperature dependences of the linear alkane diffusion coefficients in helium shown in Table 2 reproduce the ex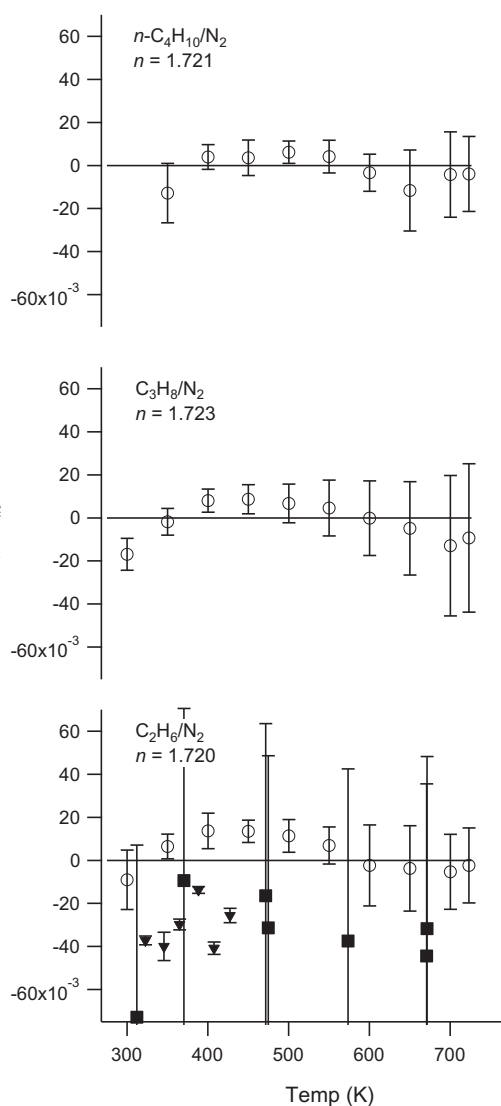perimental data well. Dunlop and Bignell have measured the low-temperature diffusion coefficients for ethane, propane, and butane in helium using a two-bulb system for temperatures ranging from 280 K to 400 K [17]. These are shown in Fig. 3 as solid circles. The present data tend to be slightly lower than these reference values for all three hydrocarbon systems, though most of the overlapping data are consistent to within experimental errors. In addition, Frost measured these diffusion coefficients for temperatures up to 766.9 K utilizing a modified Stefan cell [18,20]. Those results show slightly more scatter than the present data and are generally consistent with both the present results and the two-bulb reference values from Dunlop and Bignell where the respective temperatures overlap (up to 400 K). It should be noted that the diffusion coefficients are slightly dependent on the analyte mole fraction and that the alkane concentrations employed by Frost were much higher than the dilute samples used in the present work and by Dunlop and Bignell.

The exponent of the temperature dependence, m, for the present systems (Table 2), lie in the range m = 1.64–1.69. This is very similar to the temperature dependence for other systems in helium [10,14,17] and is somewhat lower than observed for diffusion coefficients of the hydrocarbons in nitrogen. Fits of the data from

Dunlop and Bignell's series of measurements of D for several hydrocarbons and fluorocarbons in He for T = 280–400 K show values of m = 1.63–1.67, with m = 1.659, 1.650, and 1.655 for diffusion of ethane, propane, and n-butane, respectively. Katsanos and Karaiskakis used RF-GC to measure the diffusion of ethane in He from T = 296.7–447.3 K. The present work reproduces these values well, and those authors obtained a temperature exponent m = 1.60. Presently, we find a slightly larger value for m. Tang and Hawkes utilized a chromatographic peak broadening technique to measure the diffusion of propane in helium for temperatures up to 333 K [19]. These results are shown as +'s in Fig. 2 but are not included in the deviation plots. Note in the figure that these data appear to overlap the n-butane/He data but should be compared to the propane/He data. The present results deviate significantly from the Tang and Hawkes peak-broadening results, which are also substantially lower than the two-bulb results of Dunlop and Bignell. In addition, the data of Tang and Hawkes correspond to a temperature exponent of m = 3.0805, which differs widely from that observed for other hydrocarbon–helium systems, including the present system.

4.2. Diffusion of hydrocarbons in nitrogen

As in helium, the simple temperature dependence described in Table 2 reproduces the measured diffusion coefficients for ethane, propane, and n-butane in nitrogen well. The temperature exponents m (Eq. (2)) for these systems vary little, ranging from 1.720 to 1.723 for all three systems.

Karaiskakis and Katsanos have measured the ethane–N_2 binary diffusion coefficients as part of a larger series of hydrocarbon diffusion measurements using a similar RF-GC system to the present apparatus [11]. These results are shown in Fig. 4 as solid inverted triangles. The diffusion coefficients in the present work is higher than these results throughout the common temperature range with only slight variations.

Wakeham and Slater measured the binary diffusion coefficients for all three hydrocarbons considered presently at temperatures from 313.7 K to 671.3 K using chromatographic peak broadening [16]. These results are shown as closed squares in the figures. Particularly for propane and n-butane, the present results deviate widely from those values with the deviations increasing rapidly as temperature increases. The deviations are shown in Fig. 4 only for ethane–N_2; the other deviations are too large to effectively show with a reasonable scale but are evident in Fig. 2. Wakeham and Slater used fits of the form in Eq. (2) and found decreasing exponents m = 1.73, 1.66, and 1.61 for ethane, propane, and butane (in N_2), respectively. With the exception of ethane, these are substantially different than the values of m observed in the present work (Table 2). In particular it should be noted that the present measurements do not reproduce the substantial decrease in the value of m with increasing mass observed by Wakeham and Slater [16].

The temperature-dependence exponents for diffusion coefficients in N_2 is found to be larger than that for coefficients in helium. Presently, we find exponents to be $m \approx 1.72$, larger than for typical hydrocarbons in helium. This is consistent with the temperature-dependence data measured by Katsanos and Karaiskakis for several linear hydrocarbons in both N_2 and He at temperatures up to 459.0 K [11] and is similarly expected from kinetic theory [21,22].

4.3. Pressure scaling

In the reporting of low-pressure (density) binary diffusion coefficients, it is customary to scale the diffusion coefficients linearly to 1.013 bar (1 atm) [9]. Dunlop and coworkers, in a series of studies

of the diffusion of inert gases, hydrocarbons, fluorocarbons, and other small gases [23–26] have examined the pressure dependence of binary diffusion coefficients in helium at 300 K and 323 K at pressures from 1.01 bar to 9.09 bar. In these systems, the pressure-dependent diffusion coefficients were fit with a functional form

$$PD_{12} = (PD_{12})_0(1 + \theta P),\qquad(3)$$

where P is the pressure and D_{12} is the binary diffusion coefficient. For diffusion of argon [23], neon [23], nitrogen [24], and oxygen [24], absolute deviations from linear pressure scaling $|\theta|$ were found to be less than 0.02% bar^{-1}. As analyte size increased, the deviation from linear behavior, θ, was found by those authors to increase substantially. Based on these results, and the typically ≈ 3.6 bar experimental pressure used in this work, the expected variation in the 300 K diffusion coefficients as a result of the pressure scaling would be as high as 1.4% for n-butane (which is not reported due to adhesion, as described in the following section).

At higher temperatures, pressure-dependent data are extremely limited. Arora and Dunlop have studied the pressure dependence of the binary diffusion coefficients of argon, nitrogen, oxygen, and carbon dioxide in helium at both 300 K and 323 K [25] and found that deviations were small but consistently increase with temperature, switching signs in the case of argon and nitrogen. Harstad and Bellan have developed corresponding states expressions for the temperature- and pressure-dependence of diffusion coefficients for these systems in He [21]. Although their work shows substantial deviations from linearity at higher pressures, under the present conditions the deviation from linearity in the pressure scaling is calculated to be <0.2% at 300 K and decreases with increasing temperature. We have elected to report our values scaled linearly to 1.013 bar (1 atm) with no deviation (i.e., θ = 0). Raw diffusion coefficients and measurement pressures are provided in Supplemental material.

4.4. Uncertainties at temperature extremes

At the extreme ends of the temperature ranges, we have observed deviations from the simple dependence shown in Eq. (2). Although this simple form is not exact, it has been found previously to effectively reproduce temperature variations in a wide range of systems [11,27,17,15].

At the upper end of our temperature range (near 700 K), the large reported uncertainties are due to two major factors. First, the temperature variation along the curved diffusion tube is greatest at the higher temperatures due to a vertical temperature gradient in the Oven GC (Fig. 1) that houses the column. Second, the fast diffusion of the analyte at higher temperatures allows only a small number of flow reversals (and thus points for analysis) before nonidealities influence the ability to determine the diffusion coefficient. Both of these issues are discussed in greater detail in Ref. [10].

Another possible uncertainty, particularly for larger hydrocarbons, is decomposition of the analyte. Decomposition would lead to the formation of smaller products that diffuse faster than the desired analyte but cannot be differentiated in the flame ionization detector. We expect to see these as a characteristic "tailing" of the positive reversal peaks, and such deviations have been observed in preliminary experiments for larger hydrocarbons. In the present systems, we did not observe significant tailing in the positive reversal peaks at any temperature, and the data are fit well by a temperature dependence of the form aT^m.

At the lower temperatures, we observed deviations from the simple temperature dependence in n-butane that are not consistent with other small hydrocarbons studied in our laboratory or our previous work on noble gases. These deviations may be

attributed to adhesion of the analyte on the wall of the diffusion tube leading to a lag in the output concentration relative to simple diffusion. The adhesion lag has a significant impact on the measured diffusion coefficients, in particular on the linearity of the $\ln s\tau^{3/2}$ versus $1/\tau$ plot. We have observed this effect in preliminary studies of longer linear hydrocarbons and have found that the deviation increases both in magnitude and in the temperatures at which the adhesion lag must be considered. In these cases, the lag is apparent as tailing in the shapes of the reversal peaks. We have chosen not to report diffusion coefficients at a given temperature and pressure in which adhesion lag is presumed to affect the measured diffusion coefficients. Presently, only the 300 K diffusion coefficient for *n*-butane in N_2 has been omitted as noted on Table 1.

In general, a slight bias (<2%) at low temperatures may be observed in the analyte-helium measurements relative to the reference data. A similar slight bias was observed previously [10] for the diffusion of methane in He. The effective length of the tube used in this work was determined using the best reference data available, that of dilute argon in helium at 300 K [13,12] using thermal conductivity detection. It is unknown if the observed low-temperature bias is due to differences in measurements with the flame ionization detector or other factors.

5. Conclusion

We report diffusion coefficients for ethane, propane, and *n*-butane in helium and nitrogen at temperatures ranging from 300 K to 723 K. In He, the measured data reproduce previous experiments well over the entire temperature range. In nitrogen, we find that the diffusion coefficients for propane and *n*-butane deviate substantially from previous work, with corrections up to 16.9% for *n*-butane at 671.3 K. In addition, we find that the diffusion coefficients are well described by $D = aT^m$, where *T* is in K, and *a* and *m* are parameters. The exponent *m* is defined with good precision by the present measurements and is found to depend on the bath gas but varies less with analyte with *m* being larger for diffusion in helium, consistent with kinetic theory. Future work will focus on additional hydrocarbon diffusion coefficients and the effects of decomposition and surface adhesion on measured diffusion coefficients.

Acknowledgment

Appendix A. Supplementary material

Raw binary diffusion coefficients and their corresponding measurement pressures for all data used to generate Table 1 are provided as supplemental material.

Supplementary data associated with this article can be found, in the online version, at http://dx.doi.org/10.1016/j.combustflame.2012.04.015.

References

[1] H. Wang, Chem. Phys. Lett. 325 (2000) 661–667.
[2] M.K. Mishra, R. Yetter, Y. Reuven, H. Rabitz, M.D. Smooke, Int. J. Chem. Kin. 26 (1994) 437–453.
[3] A.T. Holley, Y. Dong, M.G. Andac, F.N. Egolfopoulos, Combust. Flame 144 (2006) 448–460.
[4] C.S. McEnally, D.M. Ciuparu, L.D. Pfefferle, Combust. Flame 134 (2003) 339–353.
[5] N.J. Brown, K.L. Revzan, Int. J. Chem. Kin. 37 (2005) 538–553.
[6] N.J. Brown, L.A.J. Bastien, P.N. Price, Progr. Energy Combust. Sci. 37 (2011) 565–582.
[7] K. Chae, A. Violi, J. Chem. Phys. 134 (2011) 044537.
[8] N. Katsanos, G. Karaiskakis, J. Chromatog. A. 237 (1982) 1–14.
[9] G. Karaiskakis, D. Gavril, J. Chromatog. A. 1037 (2004) 147–189.
[10] W.S. McGivern, J.A. Manion, J. Chromatog. A. 1218 (2011) 8432–8442.
[11] N. Katsanos, G. Karaiskakis, J. Chromatog. A. 254 (1983) 15–25.
[12] W.A. Wakeham, A. Nagashima, Measurement of the Transport Properties of Fluids, Experimental Thermodynamics, vol. III, Blackwell Scientific, Oxford, 1991.
[13] P.S. Arora, I.R. Shankland, T.N. Bell, M.A. Yabsley, P.J. Dunlop, Rev. Sci. Instrumen. 48 (1977) 673.
[14] G. Karaiskakis, N.A. Katsanos, A. Niotis, Chromatographia 17 (1983) 310–312.
[15] D. Gavril, K.R. Atta, G. Karaiskakis, Fluid Phase Equilib. 218 (2004) 177–188.
[16] W.A. Wakeham, D.H. Slater, J. Phys. B: At. Mol. Phys. 6 (1973) 886.
[17] P.J. Dunlop, C.M. Bignell, J. Chem. Phys. 93 (1990) 2701–2703.
[18] A.C. Frost, A Method for the Measurement of Binary Gas Diffusivities, Ph.D., Columbia University, New York, NY, 1967.
[19] F.T. Tang, S. Hawkes, J. Chem. Eng. Data 29 (1984) 124–125.
[20] A.C. Frost, E.H. Amick, Ind. Eng. Chem. Fundam. 12 (1973) 129–133.
[21] K. Harstad, J. Bellan, Ind. Eng. Chem. Res. 43 (2004) 645–654.
[22] J. Bzowski, J. Kestin, E.A. Mason, F.J. Uribe, J. Phys. Chem. Ref. Data 19 (1990) 1179–1232.
[23] G.R. Staker, P.J. Dunlop, Chem. Phys. Lett. 42 (1976) 419–422.
[24] T.N. Bell, I.R. Shankland, P.J. Dunlop, Chem. Phys. Lett. 45 (1977) 445–448.
[25] P.S. Arora, P.J. Dunlop, J. Chem. Phys. 71 (1979) 2430–2432.
[26] P.J. Dunlop, C.M. Bignell, J. Chem. Phys. 104 (1996) 296–299.
[27] R.C. Reid, J.M. Prausnitz, B.E. Poling, The Properties of Gases and Liquids, forth ed., McGraw-Hill Companies, 1987.